RoMEO: An experimental mobile robot for path planning

Hugo G. González-Hernández[1*]; David Chillón-Escárcega[2]; Federico Zavaleta-Chimal[2] and Eduardo R. Mondragón-Parra[3]

[1] Centro de Investigación Científica y de Educación Superior de Ensenada, CICESE, Km. 107 Carr. Tijuana-Ensenada, CP 22860, Ensenada B. C. México. hgonz@cicese.mx
[2] Escuela de Ingeniería, Universidad La Salle, Benjamín Franklin 47, Col. Condesa. CP 06140, México, D. F. México. chillonov79@yahoo.com.mx, chimal15@avantel.net
[3] Delphi Automotive Juarez Operations. Ave. Antonio J. Bermúdez 1230 CP 2470, Cd. Juarez, Chih., México, eduardo.mondragon@delphiauto.com

Abstract. *In this paper, the design and construction of an omnidirectional mobile robot for experimental path planning tasks, is described. The autoguided vehicle (AGV) is called RoMEO (Omnidirectional Experimental Mobile Robot) and was designed and constructed to evolve in a controlled environment. A top view image of a room in which there are some obstacles to be avoided is obtained. Then, taking into account smoothness and length restrictions, a previously developed path-planning scheme [2] is applied to determine the optimal path between two points in the workspace. This path is codified into traction and steering commands for the corresponding DC motors in the AGV. The resulting command signals are fed into a transmitter, connected directly to a personal computer, and sent via RF to a receiver in the AGV.*

Keywords. Path Planning, Skeleton, Auto Guided Vehicles, Real time systems, Mobile Robots.

1. Introduction

The interest on AGV's has grown because of the variety of its industrial, mining and service applications. Actually, it is possible to develop an AGV with a sensorial control for moving in a structured environment, or to react in an unknown or variable environment [1]. However, correction mechanisms for robot position are not autonomous, *i.e.* it is required external information to measure the position error introduced by wheel sliding. One of the problems in the design of autonomous robots is the automatic path planning for navigation in an unknown or variable environment along an optimized free collision path using visual information (see Fig. 1).

Fig. 1 Desired trajectory

In this paper the design and construction of a mobile robot for path planning is described in detail. The electromechanical design of the robot was done to avoid possible collisions with obstacles. Particularly those caused by turns in 4 or 3-wheels designs. The main idea in this design was to solve this problem using an omnidirectional approach, *i.e.* the robot consists of only one-wheel, which is able to give the robot the direction, orientation, and motion needed to track some desired trajectory. It does not have holonomic restrictions
The mobile robot is controlled via a personal computer. We use a previously reported method for path planning, which uses the information from the top view of a camera to provide the optimal collision-free path between an initial and a goal point. The method considers length and smoothness restrictions. No other sensor is used in this approach.
The optimal trajectory is codified into commands for the tracking and rotation motors of the robot. This codified trajectory is fed into a transmitter module, which is connected to the parallel port of the personal computer, and sent via RF to the receiver module in the robot.
The paper is organized as follows: Section 2 deals with a brief analysis of the kinematics and dynamics of the robot. Section 3 is devoted to the RF communications system; later on section 4, we describe the power management and control for the motors in the robot.

2. The mobile robot

This section is dedicated to the analysis of the structural, kinematics and dynamics behavior of an omnidirectional mobile robot, designed and constructed by the authors. The robot has two DC motors: a traction motor and a steering motor and it may move in any direction on the horizontal plane.

2. 1 Structural analysis

In Fig. 2 two significant zones in the mobile robot structure are shown. The analysis for zone 1 turns out to be quite simple, because the applied load is considered axial

[*] This work was partially done when the author was at the Research Center in Universidad La Salle, Mexico City.

to the pole and also static [3]. Consider the total load of the three poles shown in Table 1.

Component	Mass (g)
Base	280
Bolts	(3)(6)=18
Motors	170.5
Electronic Circuit	100
Total	668.5

Table 1. Total load

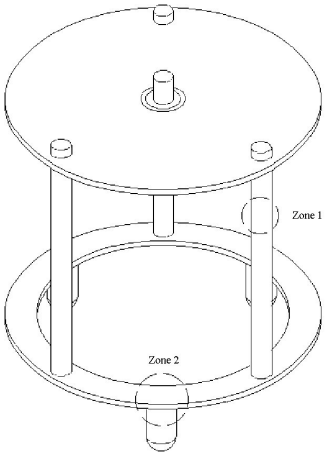

Fig. 2 RoMEO structure

The total load is 6.558N. The load of a single pole is: W_{pole}=2.186 N and its area is A_{pole}= 1.039e-0.4m^2. Thus, the work effort turns out to be 21.04 KPa. Comparing it with the maximum effort for aluminum (121 MPa), the structure is robust enough.

To analyze zone 2 consider Fig. 3

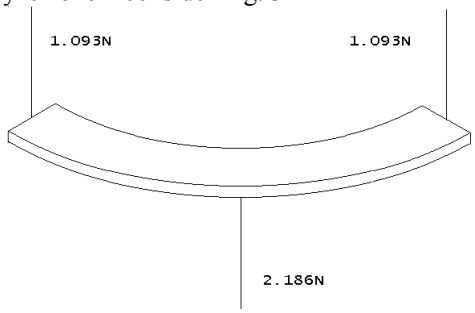

Fig. 3 Actuating loads in zone 2

We have 1.093 N pole loads giving a reaction 2.186 N force is the bearing. The application distances of the forces were obtained using the model in Fig. 4. For r=0.09 m and ang=p/6, knowing Y=((0.09)(6)sin(p/6))/p=0.0859 m; r-Y=4.056E-0.3 m; X=0.05 m; 2X=0.01 m.

With these distances known we can obtain the diagrams of shear forces and momentum, which are shown in Fig. 5. The normal force is $\sigma=M_c/I$=-102.47KPa, the shear stress is $\tau_{max} = T/Q$; $Q = bh^2/(3+1.8(h/b)) = 46.55$ KPa. Using the Mohr circle [ref] we have found the extreme effort τ_1=46.55KPa + 102.47 KPa/2 = 97.785KPa. Again, the structure is robust enough.

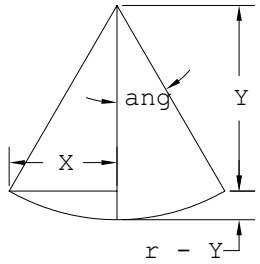

Fig. 4 Application distances of the forces

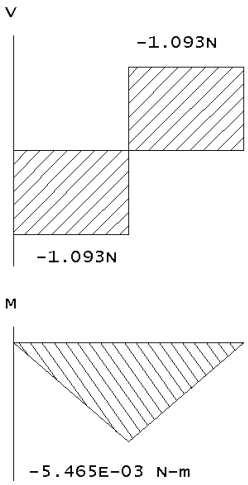

Fig. 5 Diagram of shear forces efforts and momentum

2.2 Kinematics analysis

For direct kinematics analysis we have θ (steering motor angle) and γ (traction motor angle) as independent variables. As dependent variables we have x_1, y_1, and r as a parameter. Consider Fig. 5.

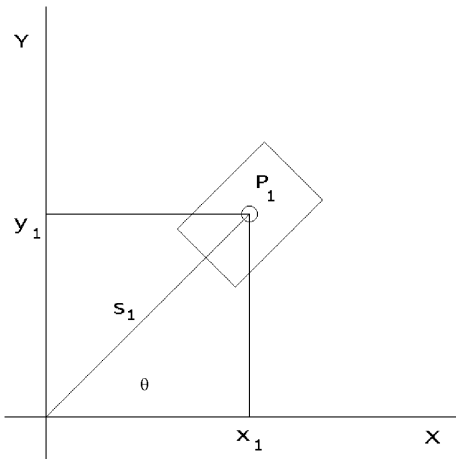

Fig. 6 Kinematics scheme

The position command is point $P_1(x,y)\in\Re^2$. Let S_1 be the trajectory, we consider there is no slippage between wheels and floor and initially the wheel axis is on line with the X axis, then

$$|S_1| = \gamma_1 r = \sqrt{x_1^2 + y_1^2} \qquad (1)$$

$$S_1 \cos\theta_1 = x_1 \quad (2)$$
$$S_1 \sin\theta_1 = y_1 \quad (3)$$

where $0 \le q_1 < 360°$ and $-a<g_1<a$. From equations (1), (2) and (3):

$$x_1 = \gamma_1 r \cos\theta_1 \quad (4)$$
$$y_1 = \gamma_1 r \sin\theta_1 \quad (5)$$

where (4) and (5) are the direct kinematics equations. For inverse kinematics:

$$\gamma_1 = \frac{S_1}{r} = \frac{\sqrt{x_1^2 + y_1^2}}{r} \quad (6)$$

$$\theta_1 = \cos^{-1}\left(\frac{x_1}{\sqrt{x_1^2 + y_1^2}}\right) \quad (7)$$

The general case for finding the location of the robot centroid:

$$x_{n+1} = x_n + (\gamma_{n+1} - \gamma_n) r \cos\theta_n \quad (8)$$
$$y_{n+1} = y_n + (\gamma_{n+1} - \gamma_n) r \sin\theta_n \quad (9)$$

for a point P_n, n=1, 2,3,...

2.3 Analysis of the Dynamics

It is considered that the center of mass is over the shaft, the robot requires balancing for this consideration (Fig. 7)

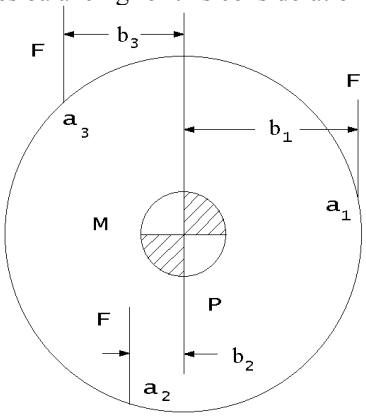

Fig. 7 Free body diagram

We have P=3F and F=($-b_1+b_2+b_3$)=0. Thus $b_1=b_2+b_3$. The equations mentioned above are accomplished supported upon a geometric analysis. In a_1, a_2, a_3, there is the same friction force F, provided that weight is distributed between the three poles uniformly. Besides, they are bearings of the same type, see Fig. 8 and Fig. 9.

For the dynamical model we consider q = [θ γ] as generalized coordinates. Variables and parameters in Table 2 were considered. We have used a classical approach to find the dynamics of the robot. We obtained the Lagrangian of the system [4]

$$L = T - U = \frac{1}{2} M(\dot{x} + \dot{y}) + \frac{1}{2} I_1 \dot{\theta}^2 + \frac{1}{2} I_2 \dot{\gamma}^2 \quad (10)$$

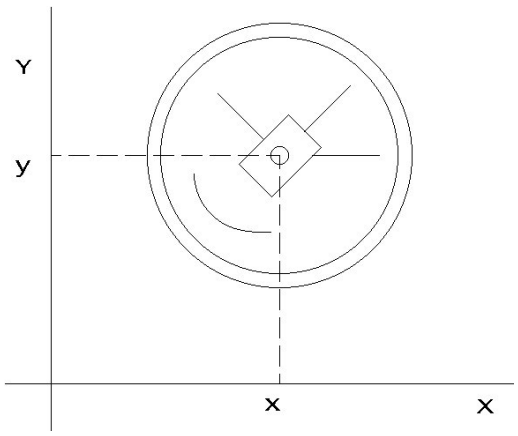

Fig. 8 RoMEO in the plane

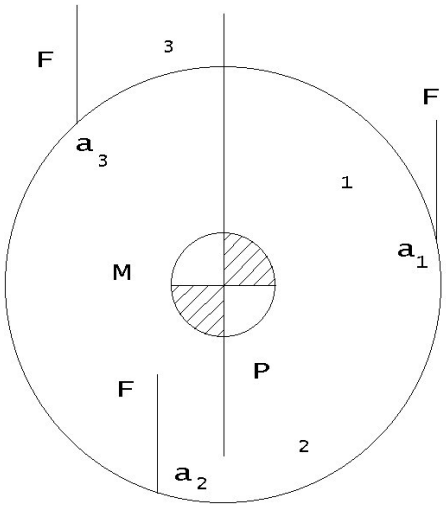

Fig. 9 Traction wheel

T_1	Steering motor torque
T_2	Traction motor torque
X	Position coordinate
Y	Position coordinate
θ	Steering motor angle
γ	Traction motor angle
M	Robot mass
I_1	Inertia with respect to θ
I_2	Inertia with respect to γ
R	Traction wheel radius

Table 2. Variables and parameters

and consider the Rayleigh function

$$D = \frac{1}{2} b_1 \dot{\theta}^2 + \frac{1}{2} b_2 \dot{\gamma}^2 + \frac{1}{2} b_3 (r\dot{\gamma})^2 \quad (11)$$

Thus, the dynamics equations of the system become:

$$\begin{aligned} &I_1 \ddot{\theta} + b_1 \dot{\theta} = T_1 \\ &(Mr^2 + I_2)\ddot{\gamma} + (b_2 + b_3 r^2)\dot{\gamma} = T_2 \end{aligned} \quad (12)$$

Choosing the state vector $x = [\theta \ \dot{\theta} \ \gamma \ \dot{\gamma}]$ (12) can be expressed as:

$$\begin{bmatrix} \dot{x}_1 \\ \dot{x}_2 \\ \dot{x}_3 \\ \dot{x}_4 \end{bmatrix} = \begin{bmatrix} 0 & 1 & 0 & 0 \\ 0 & -\frac{b_1}{I_1} & 0 & 0 \\ 0 & 0 & 0 & 1 \\ 0 & 0 & 0 & -\frac{b_2 + b_3 r^2}{Mr^2 + I_2} \end{bmatrix} \begin{bmatrix} x_1 \\ x_2 \\ x_3 \\ x_4 \end{bmatrix} + \begin{bmatrix} 0 & 0 \\ \frac{1}{I_1} & 0 \\ 0 & 0 \\ 0 & \frac{1}{Mr^2 + I_2} \end{bmatrix} \begin{bmatrix} \tau_1 \\ \tau_2 \end{bmatrix}$$

(13)

3. Communications system

In this section we describe the design and construction of the RF communication system, we use BASIC Stamp with TWS/RWS RF modules.

3.1 Transmitter module

In Fig. 10 it is shown the circuit connections for the transmitter, we are using a Holtek HT-640 codifier and a TWS-434 RF transmitter module, which requires only a 13-inch piece of insulated hobby wire for an effective antenna; although, we have decided to use special whip antennas for transmitter and for receiver also. These antennas provide maximum operating distance for the TWS and RWS RF modules.

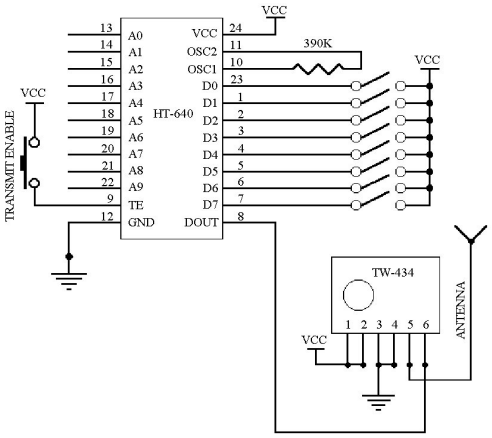

Fig. 10 Transmitter circuit

3.2 Receiver module

For the receptor we have used RWS-434 receiver module. Connections are shown in Fig 10. We decided to use the digital output because we have had better reception results. Pin 2 on the RWS-434will pulse continuously. The TWS-434 and RWS-434 are small size, and require short-range RF remote control. The transmitter output is up to 8mW at 433.92MHz with a range of approximately 400 ft (open area) outdoors. Indoors, the range is approximately 200 ft, and will go through most walls. The TWS-434 transmitter accepts both linear and digital inputs, can operate from 1.5 to 12 Volts-DC. The receiver also operates at 433.92MHz, and has a sensitivity of 3μV. The RWS-434 receiver operates from 4.5 to 5.5 V DC, and has both linear and digital outputs.

3.3 Decoder HT-640

The decoder and the encoder were chosen to use in this project because of their features. They have an operating voltage from 2.4V to 12V, and one of their main features is that they have a low standby current. We use the minimal external components with this kind of encoder and decoder.

The Holtek HT-640 encoder (Fig. 11) is a CMOS LSI for remote control system applications. It is capable of encoding 18 bits of information, which consists of *N* address bits and 18 *N* data bits. Each address/data input is externally programmable if bonded out. It is otherwise set floating internally.

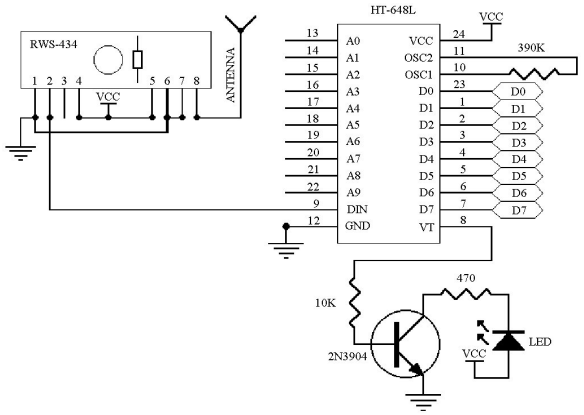

Fig. 11 Receiver circuit

The programmable address/data is transmitted together with the header bits via an RF or an infrared transmission medium upon receipt of a trigger signal. The capability to select a transmission enable (TE) trigger type or a DATA trigger type further enhances the application flexibility HT640 Encoder.

3.4 Decoder HT 648L

The Holtek HT-648L decoder provides several combinations of address and data pins in different packages. They are paired with the 318 series of encoders. The HT-648L decoder receives serial address and data from the encoder that is transmitted by a carrier using RF. It then compares the serial input data twice continuously with its local address. If no errors or unmatched codes are encountered, the input data codes are decoded and then transferred to the output pins.

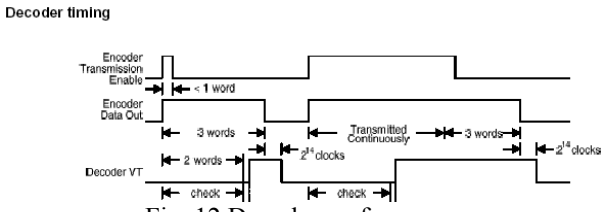

Fig. 12 Decoder performance

4. Robot motion and power control

The robot has two motors which have to be driven by the same power source and should be controlled separately. It was taken into account that due to the robot design, the power source should consist in two 6V, 1A/Hr batteries that jointly give 12V, 1Amp/Hr. We have to decrease the energy consumption in order the robot to move efficiently during long periods of time.

The robot motion is controlled with two 12V/1A DC motors driven separately the first motor is used for the traction and the second for the steering. The voltage source is provided by two 6V, 1A/Hr batteries in a serial connection for obtaining 12V, 1 A/Hr. Receiver circuit needs 4.8V, 320mA/Hr.

4.1 Motion control

A PWM driven H-Bridge is used to control both motors (see Fig. 13 for steering motor control and Fig. 14 for tracking motor control), this allows us to control the motors angular position and velocity; this helps in minimizing the error in high velocity motion. We have designed an H-Bridge using low cost IRF520 (N-channel) and IRF9520 (P-channel) MOSFET's, which satisfy the design parameters.

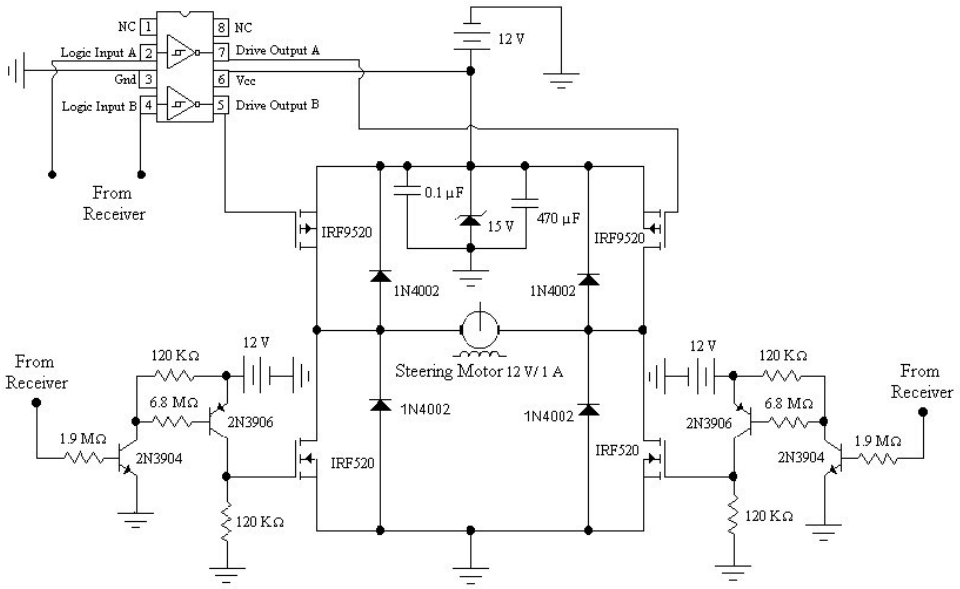

Fig. 13 Steering motor H-Bridge

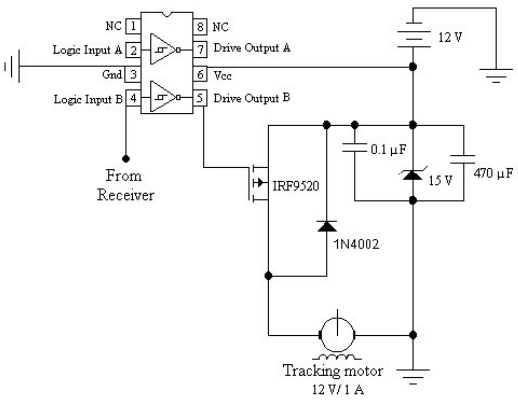

Fig. 14 Tracking motor controller

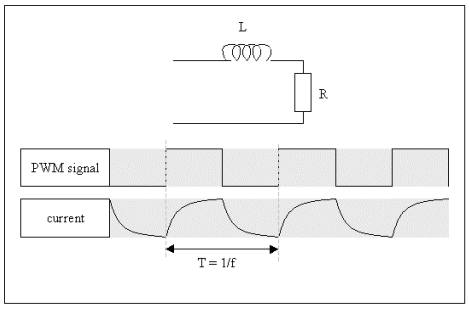

Fig. 15 Operating Frequency

An important issue to determine is the operating frequency (see Fig. 15) this frequency should be appropriate for the performance of the robot motors. The main idea is to keep

stable the current signal to avoid that the inductor of the motor could generate voltage peaks in each commutation of the PWM signal. The commutation speed was verified and both MOSFET's had commutation speed of nanoseconds order; so, this would not be limiting for the use of PWM.

4.1 Trigger circuits

The trigger circuits for the MOSFET's were designed using low signal BJT in order to minimize energy consumption (Fig. 16). We use an individual trigger controller for each MOSFET in order to keep the gates isolated from induction and noise generated for the DC motor. The BJT transistors used were 2N3904 (NPN) and its complement 2N3906 (PNP). These transistors have a maximum saturation voltage $V_{CESatmax}$ = 0.2 V and were configured to work with collector and base currents below 1 mA achieving important energy savings. Also they were chosen because they can be operated with frequencies up to 100 MHz and allow, with no limitations, the use of PWM.

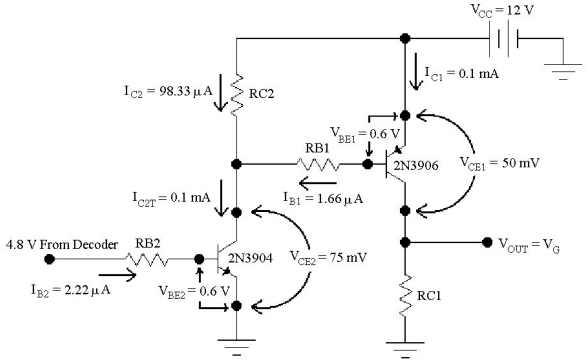

Fig. 16 Triggering circuit

5. Conclusions

Path planning in Robotics is an area in which several aspects of control, system modeling and sometimes topology are involved. Particularly, in path planning it is needed a prototype robotic system in order to experimentally test developed algorithms. There are several mobile robots in the market but usually they are high cost systems.

In this paper, the design and construction of a low cost mobile robot was described (Fig. 19). This is a flexible design and gives us the possibility of test different algorithms, including tracking landmarks with minor changes in the robotic device. As a future important issue to continue this work consists in the design of a closed loop robot control vision system to manage errors in the tracking of a desired trajectory.

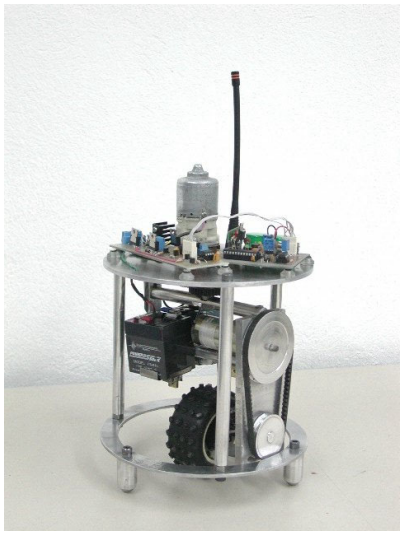

Fig. 19 RoMEO

References

[1] Latombe, Jean-Claude. (1991). *Robot Motion Planning*. Kluwer Academic Publishers.

[2] González-Hernández, H. G. (1995) "Automatic path planning for autoguided vehicles" *MSc Thesis* (in Spanish) CINVESTAV-IPN. México City, México.

[3] Kimbrell, J. (1991) *Kinematics Analysis and Synthesis*. McGraw-Hill. Singapore.

[4] Marion, J. B. (1965) *Classical Dynamics*. Academic Press, N.Y.